Effect and Distribution of Contrast Medium after Injection into the Anterior Suprachoroidal Space in Ex Vivo Eyes

Gabriela S. Seiler,[1] *Jacklyn H. Salmon,*[2] *Rebecca Mantuo,*[2] *Steven Feingold,*[3] *Paul A. Dayton,*[3] *and Brian C. Gilger*[2]

Purpose. To determine the effects and posterior distribution of injections made into the anterior suprachoroidal space (SCS).

Methods. The anterior SCS of adult porcine and canine ex vivo eyes was cannulated. Latex injections and high frequency ultrasound (50 MHz) was used to image the effect and distension of the SCS. Flow characteristics and percentage maximal distribution of microbubble contrast injection into the SCS were assessed by 2D and 3D ultrasound.

Results. Mean (SD) distension of the SCS with PBS increased from 1.57 (0.48) mm after injection of 250 μL to 3.28 (0.57) mm with 1000 μL PBS. Eyes injected at physiologic IOP had no significant difference in SCS distension. In real-time 2D ultrasound, the contrast agent flowed from the injection site to the opposite ventral anterior SCS and the posterior SCS. Contrast arrived at the opposite and posterior SCS 7.8 (4.6) and 7.7 (4.6) seconds after injection, respectively. In sagittal images, contrast was visible in 24.0%to 27.2% of the SCS; in 10 of 12 eyes, contrast reached the posterior pole of the eye. In 3D images, contrast medium occupied 39.0% to 52.1% of the entire SCS.

Conclusions. These results suggest that the SCS can expand, in a dose-dependent manner, to accommodate various volumes of fluid and that it is possible to image the SCS with ultrasound contrast. The authors' hypothesis that a single anterior SCS injection can reach the ocular posterior segment was supported. Further development of SCS injections for treatment of the ocular posterior segment is warranted. (*Invest Ophthalmol Vis Sci.* 2011;52:5730–5736) DOI:10.1167/iovs.11-7525

Diseases of the posterior segment of the eye are among the most common causes of blindness. In humans, these diseases include age-related macular degeneration, proliferative vitreoretinopathy, diabetic macular edema, and endophthalmitis. Although there are many advances in the treatment of these posterior segment diseases, the challenges of drug delivery to this part of the eye remain high.[1] Eye drops continue to be a mainstay in the treatment of ocular disease, but most topical medications do not penetrate the posterior segment.[2,3] Local therapy of the eye, such as periocular and intravitreal injections, has recently become popular to treat ocular disease because they minimize systemic side effects and take advantage of small tissue volumes and compartments of the eye.[4,5] Natural barriers to ocular drug penetration, such as conjunctival lymphatics, sclera, choroidal circulation, and epithelial tight junctions, limit the ability of periocular injections to reach posterior target tissues.[1,6,7] Instead, ocular posterior segment disease, such as choroidal neovascularization, macular degeneration, and retinal degeneration, are commonly treated locally by intravitreal or subretinal injections or use of sustained-release devices. However, these treatment modalities are subject to complications such as injection site hemorrhage, retinal detachment, cataract formation, endophthalmitis, elevated intraocular pressure, opacities of the visual axis, and local toxicity.[8–10] Therefore, alternative sites for drug delivery to the ocular posterior segment are needed.

Drug delivery to the suprachoroidal space (SCS), a potential space located between the choroid and the sclera,[11] avoids many of the disadvantages of other local therapies by eluding barriers such as conjunctival lymphatics and the sclera and may avoid complications associated with intraocular injections or implants. Furthermore, because the SCS is adjacent to the entire choroid and thus the ocular posterior segment, drug delivery using the SCS has the potential for wide drug distribution and for reach to posterior target tissues.

Recently, studies have demonstrated promise in the use of the SCS as a site for drug delivery to the eye. Use of the SCS as a drug delivery site was first described by Einmahl et al.,[12] who placed a poly-ortho ester–sustained drug delivery system in the SCS in rabbits and demonstrated sustained delivery in the SCS for 3 weeks.[12] Ultrasound was used to track the distribution of injected material in this study.[12] In 2006, Olsen et al.[13] described the use of a fiberoptic microcannula to access the SCS in a pig with few complications.[13] Sustained ocular drug delivery of triamcinolone to the SCS was demonstrated using this cannula, with resulting low systemic drug levels. A volume of 12 μL triamcinolone was placed into the SCS by use of the flexible catheter, and no side effects were noted with the cannulation procedure or drug; after the cannula was removed, the SCS was found to return to a normal configuration.[13] Subconjunctival infusion (1 and 10 μL/min) of gadolinium-diethylenetriaminopentaacetic acid (Gd-DTPA) in rabbits resulted in no ocular posterior segment distribution, whereas anterior intrascleral infusion resulted in rapid entry of Gd-DTPA into the SCS. The Gd-DTPA was then demonstrated to widely distribute to the posterior segment of the eye by way of the SCS.[6] In another study in rabbits, up to 100 μL fibrin glue was injected into the SCS, resulting in minimal toxicity and complications.[14] Preliminary studies have also demonstrated that large biological proteins, such as a human antibody (i.e., bevacizumab), injected into in the SCS in a pig model resulted

From the Departments of [1]Molecular Biomedical Sciences and [2]Clinical Sciences, North Carolina State University, Raleigh, North Carolina; and the [3]Joint Department of Biomedical Engineering, University of North Carolina at Chapel Hill and North Carolina State University at Raleigh, North Carolina.

Submitted for publication March 8, 2011; revised April 26, 2011; accepted June 1, 2011.

Disclosure: **G.S. Seiler**, None; **J.H. Salmon**, None; **R. Mantuo**, None; **S. Feingold**, None; **P.A. Dayton**, Targeson, Inc. (C); **B.C. Gilger**, None

Corresponding author: Gabriela S. Seiler, Department of Molecular Biomedical Sciences, North Carolina State University, 1052 William Moore Drive, Raleigh, NC 27607; gsseiler@ncsu.edu.

in no inflammation, whereas a similar dose injected intravitreally resulted in granulomatous vasculitis and vitreitis.[15] Finally, the effectiveness of drug delivery to the SCS was demonstrated in a study in which a sustained-release matrix-reservoir cyclosporine device that was placed in the SCS resulted in long-term control of uveitis in a naturally occurring model of autoimmune uveitis.[16] Therefore, the SCS route of delivery may offer a unique avenue for future routine injections that are safe and effective in targeting retinal and macular diseases.

To further develop the SCS as a site for drug delivery, it is important to determine whether injections of medications into the anterior SCS, the most accessible location of the SCS, will allow distribution of the drug to the posterior targeted tissue. The SCS can be accessed through a small sclerotomy or by microneedles placed 4 to 6 mm posterior to the limbus, but the amount of drug distribution to the ocular posterior segment that can be achieved from this anterior injection location is not known. Recently, Patel et al.[17] described the use of hollow microneedles to precisely inject drugs into the SCS. In this study, volumes up to 35 μL prototype drugs of particle sizes up to 1000 nm were injected into the porcine SCS. These injections resulted in a 7% distribution to the posterior SCS.[17] However, appropriate injection volumes, area of drug distribution, and effect on the SCS of injections must be further evaluated. Furthermore, the duration of drug delivery and the ability of the drug to reach target tissues, especially the retina, must be determined for each drug and formulation.

The purpose of this study was to evaluate injections into the anterior SCS to determine the effect and distribution to the posterior SCS and to determine whether target tissues can be reached. In this study, injection volumes, acute effects of injections on the SCS, and flow characteristics of injections in the SCS were determined.

Methods

Suprachoroidal Injection Technique

Adult porcine ex vivo eyes (Animal Technologies, Tyler, TX) were collected and shipped overnight on ice. Canine ex vivo globes were collected at a local animal shelter immediately after euthanatization and transported on ice. All globes were used within 24 hours of collection. Each globe was cleaned of excess periocular tissue, including conjunctiva, extraocular muscle, and orbital fat. Canine and porcine eyes are similar in size (e.g., canine vitreous humor volume is approximately 1.7 mL whereas porcine vitreous volume is slightly higher at 2.0 mL[18,19]), and, therefore, the procedures described are applicable to each type of eye. A 2-mm full-thickness scleral incision was made 5 mm posterior to the superior limbus to expose the SCS. A 27-gauge cannula (Anterior Chamber Cannula; BD Visitec, Waltham, MA) was placed 1 mm into the SCS through the scleral incision with the opening of the cannula directed posteriorly. Cyano-acrylate tissue adhesive (Pacer Technology, Rancho Cucamonga, CA) was used to seal the sclera incision and fixate the cannula to the external sclera.

Latex Distribution

Porcine and canine eyes were allowed to warm to room temperature for 30 minutes and then were injected with undiluted liquid anatomic latex (Carolina Biological Supply Company, Burlington, NC) through the 27-gauge cannula placed in the SCS. The liquid latex was injected until injection resistance developed or when disruption of the cyano-acrylate incision seal and reflux of latex through the scleral incision occurred. An injection of approximately 1000 μL latex was required. Globes were then fixed in 10% buffered formalin (Fisher Scientific, Kalamazoo, MI) for 48 hours and sectioned either sagittally or in quadrants (i.e., flat mount) after removal of the ocular anterior segment. The retina and choroid were then removed, exposing the latex in the SCS and the sclera. High-resolution digital photographs (Nikon D200, AF-S DX Micro NIKKOR 85mm f/3.5G ED VR Lens; Nikon USA Inc, Melville, NY) of the eyes were analyzed using image analysis software (Elements 4.0, Adobe Photoshop, San Jose, CA; ImageJ software [developed by Wayne Rasband, National Institutes of Health, Bethesda, MD; available at http://rsb.info.nih.gov/ij/index.html]) to determine overall percentage area of distribution of latex to the entire SCS. Results were reported as mean (± SD) of percentage SCS distribution.

SCS Distension

Ex vivo canine and porcine eyes were used for this study. SCS cannulation was performed as described earlier. During the injection of 250, 500, 800, and 1000 μL ($n = 6$ eyes for each volume) of 0.9% phosphate-buffered saline (Fisher Scientific, Fair Lawn, NJ), high-frequency (50 MHz) ultrasound (E-technologies, Bettendorf, IA) was used to image the effect and distension of the injections on the SCS in real time. The ultrasound probe was positioned immediately over the injection site so that the adjacent sclera, SCS, and ciliary body/choroid were imaged in real time during the injection. Images were collected, and the maximal distance that the SCS was distended when injected with PBS was measured with internal calipers of the ultrasound. Results were reported as mean ± SD of SCS separation in millimeters of six eyes at each PBS volume.

To determine the effect of physiologic intraocular pressure (IOP) on SCS distension after injection and to determine the changes of IOP after SCS injection, this study was repeated in porcine ex vivo eyes ($n = 4$ per injection volume). After placement of the catheter in the SCS as described, a 27-gauge needle was placed through the limbus into the anterior chamber, and cyano-acrylate tissue adhesive was used to seal the limbal incision. The needle was connected with 0.9% saline-filled tubing to a pressure transducer (MedEx LogiCal Transducer, Model MX960; MedExSupply Medical Supplies, Monsey, NY) and an electronic monitor, allowing for continuous measurement of IOP. Immediately before injection of 250, 500, 800, or 1000 μL PBS into the SCS, the IOP was increased to 15 mm Hg by injection of 0.9% saline through the 27-gauge anterior chamber needle. Maximal distension of the SCS was measured and reported as described using internal calipers of the ultrasound. The IOP (in mm Hg) at the time of maximal SCS distension was recorded for each injection volume and reported as mean change in IOP (±SD) mm Hg.

Two-Dimensional Ultrasound Contrast Imaging of SCS

Porcine ex vivo eyes were used for this study. Using contrast-enhanced ultrasound (Mylab70; Biosound Esaote, Inc., Indianapolis, IN), 250, 500, and 800 μL microbubble ultrasound contrast agent (Targestar-P, Targeson Inc., San Diego, CA) was injected into the anterior suprachoroidal space through 27-gauge cannulas placed as described earlier. In real time, observations were recorded, including flow characteristics of the contrast agent in the SCS. Percentage of maximal distribution in the SCS of contrast agent was determined in the sagittal ultrasound plane using image analysis software (Elements 4.0 [Adobe Photoshop]; ImageJ 1.42q). Results were reported as mean (± SD) of percentage SCS distribution of four eyes at each contrast agent volume. Using contrast medium detection software (Qontrast; Biosound Esaote, Inc., Indianapolis, IN), regions of interest were placed over the entire SCS and the posterior SCS, and contrast enhancement over time was measured as mean pixel intensity.

Three-Dimensional Ultrasound Contrast Imaging of SCS

Porcine ex vivo eyes were imaged using a custom 3D contrast imaging system that interfaces a computer-controlled linear motion axis with a clinical ultrasound scanner (Acuson Sequoia; Siemens Medical Solutions, Malvern, PA). A 4-MHz (4-C1) transducer and contrast imaging (Cadence CPS; Siemens Medical Solutions, Malvern, PA) were used. The porcine eye was placed in a water bath, and 250 μL microbubble

contrast medium was injected through 27-gauge catheters placed into the anterior SCS. Dynamic contrast medium inflow was observed in a midsagittal plane, followed by 3D imaging of the entire globe to assess spatial distribution of the contrast agent. Percentage of maximal distribution in the SCS of contrast agent was determined slice by slice using image analysis software (Elements 4.0 [Adobe Photoshop]; ImageJ 1.42q). Results were reported as mean (± SD) of percentage SCS distribution of 4 eyes.

Statistical Analysis

Statistical analysis of the data was performed using computerized software (JMP Statistical Discovery Software, vs 8.0; SAS Inc., Cary, NC). Differences in SCS distension, distribution of latex, distribution of contrast media, and contrast medium enhancement were analyzed using analysis of variance (ANOVA) with Tukey's HSD test. Differences between species were analyzed using an unpaired *t*-test. Significance was set at $P \leq 0.05$ for all comparisons.

Results

Latex Distribution

Liquid anatomic latex was injected into the anterior SCS to determine posterior distribution from a single anterior injection. In canine eyes, latex distributed to a mean (± SD) of 39.9% ± 5.2% of the entire SCS on sagittal sections ($n = 4$) and 46.8% ± 13.1% of the entire SCS when the eyes were sectioned in quadrants ($n = 4$; Fig. 1). In porcine eyes, latex distributed to a mean (± SD) of 54.8% ± 15.4% of the SCS in sagittal sections ($n = 4$) and 42.1% ± 4.3% of the SCS in eyes sectioned in quadrants ($n = 4$; Fig. 1). There were no significant differences between species or sectioning techniques in area of distribution. Latex reached the SCS adjacent to the area centralis (i.e., macula) in 9 of 16 (56%) eyes (Fig. 1).

SCS Distension

High-frequency ultrasound was used to image the anterior SCS during injection with PBS. The metallic tip of the catheter was visualized in the SCS on the ultrasonic image. On injection, the SCS rapidly expanded locally, then dissected posteriorly (Fig. 2). As expected, the lower volumes of injection resulted in less distension of the SCS. In the canine eyes, maximum mean (± SD) distension of the SCS from injection with 250 μL PBS (1.25 ± 0.07 mm) was significantly lower than the maximum distension created from 500 μL PBS (2.25 ± 0.07 mm; $P = 0.02$), 800 μL PBS (2.25 ± 0.21 mm; $P = 0.02$), and 1000 μL PBS (2.7 ± 0.28 mm; $P = 0.005$; ANOVA with Tukey's HSD; Fig. 3). In the porcine eyes, maximum mean (± SD) distension of the SCS from injection with 250 μL PBS (1.57 ± 0.48 mm) was significantly lower than the maximum distension created from 800 μL PBS (2.98 ± 0.37 mm; $P = 0.002$), and 1000 μL PBS (3.28 ± 0.57 mm; $P = 0.0002$). Furthermore, the mean distension of the SCS from injection with 500 μL PBS (2.57 ± 0.52 mm) was significantly lower than the mean distension created from 1000 μL PBS ($P = 0.036$; ANOVA with Tukey's HSD; Fig. 3). There were no significant differences in

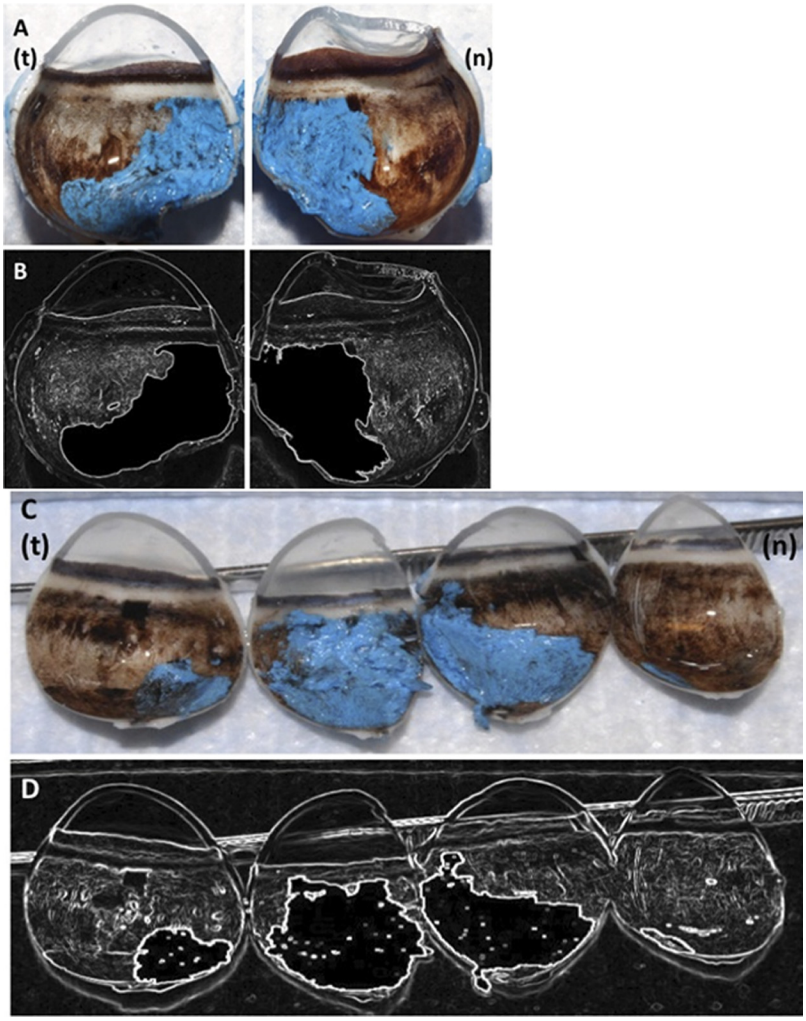

Figure 1. Temporal (t) and nasal (n) sagittal sections of a canine globe showing the suprachoroidal distribution of a single injection of blue latex in color (**A**) and in the "edges" function of ImageJ software (**B**). Canine globe sectioned in quadrants demonstrating distribution of blue latex in the SCS in color (**C**) and in the "edges" function of ImageJ software (**D**).

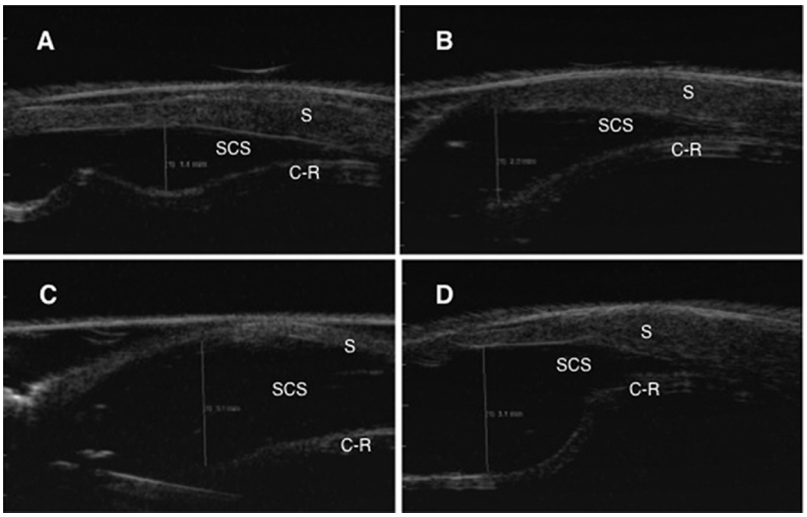

FIGURE 2. High-frequency ultrasound (50 MHz) images demonstrating the distension of the SCS in porcine eyes after injection with 250 μL (**A**), 500 μL (**B**), 800 μL (**C**), and 1000 μL (**D**) of PBS. *Left*: anterior segment; *right*: posterior segment. S, sclera; C-R, choroid and retina.

distension of the SCS between canine and porcine eyes at any injection volume except 800 μL, at which the distance was significantly greater in the porcine eye (2.98 ± 0.37 mm) than in the canine eye (2.25 ± 0.21 mm; $P = 0.035$; Student's *t*-test; Fig. 3).

To determine the effect of physiologic intraocular pressure (IOP) on SCS distension after injection and to determine the changes of IOP after SCS injection, this study was repeated in porcine ex vivo eyes with IOPs of 15 mm Hg. In these eyes, there was no significant difference in mean (± SD) distension of the SCS between (eyes injected with 250 μL (1.65 ± 0.79 mm), 500 μL (2.8 ± 0.69 mm), or 800 μL (2.8 ± 0.92 mm; Fig. 3). There also were no significant differences in mean distension for each injection volume between eyes with IOPs at 15 mm Hg compared with the ex vivo porcine or canine eyes (Fig. 3). However, injections greater than 800 μL could not be completed because of resistance to injection from high IOPs. In fact, at maximum distension during the injection of 250 μL, IOPs were transiently (<10 seconds) elevated a mean (± SD) of 39.3 ± 16.5 mm Hg; during the 500-μL injection, IOP increased a mean (± SD) 189.5 ± 118.1 mm Hg; and during the 800-μL injection, IOP increased a mean (± SD) 285.8 ± 42.9 mm Hg.

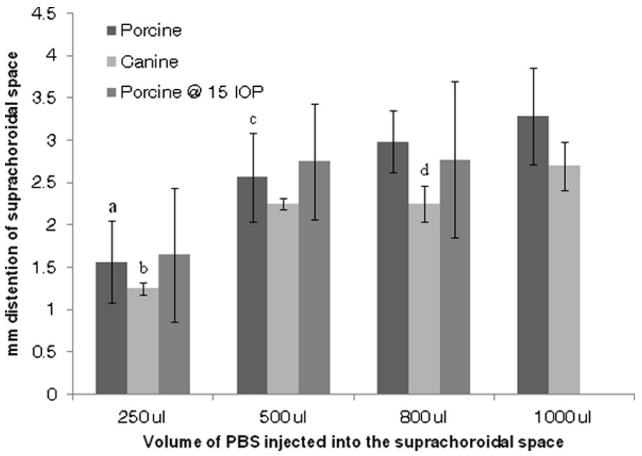

FIGURE 3. Mean ± SD distension of the SCS after injection with PBS measured using high-frequency (50 MHz) ultrasound of ex vivo porcine eyes (porcine; $n = 6$), canine eyes (canine; $n = 6$), and porcine eyes with IOP at 15 mm Hg (porcine at 15 IOP; $n = 4$). (a) Porcine eyes; mean (± SD) distension of the SCS from injection with 250 μL PBS was significantly less than the maximum distension created from 800 μL PBS ($P = 0.002$) and 1000 μL PBS ($P = 0.0002$). (b) Canine eyes; mean (± SD) distension of the SCS from injection with 250 μL PBS was significantly less than the mean distension created from 500 μL PBS ($P = 0.02$), 800 μL PBS ($P = 0.02$), and 1000 μL PBS ($P = 0.005$). (c) Porcine eyes; mean distension of the SCS from injection with 500 μL PBS was significantly less than the mean distension created from 1000 μL PBS ($P = 0.036$). (d) Mean distance was significantly less in the canine eye than in the porcine eye for the 800-μL PBS injection volume ($P = 0.035$; Student's *t*-test). There was no significant difference in mean distension of the SCS in porcine eyes at 15 mm Hg compared with the other ex vivo eyes at any injection volume.

Two-Dimensional Ultrasound Contrast Imaging of SCS. After the injection of microbubble ultrasound contrast agent into the anterior SCS of porcine eyes ($n = 4$ eyes per volume), contrast was visible initially in the SCS at the injection site and then at the opposite ventral anterior SCS and the posterior SCS. This is illustrated in Figure 4, where contrast enhancement (measured as mean pixel intensity) starts to increase first at the injection site, followed by the opposite anterior SCS and the posterior SCS. The overall mean (± SD) time after injection for contrast to appear at the opposite and posterior SCS was 7.8 ± 4.6 and 7.7 ± 4.6 seconds, respectively. This suggests that the contrast flowed in the SCS initially parallel to the limbus in the anterior suprachoroidal space as it extended posteriorly (Fig. 5; Supplementary Movie S1, http://www.iovs.org/lookup/suppl/doi:10.1167/iovs.11-7525/-/DCSupplemental). Mean (± SD) time to maximum contrast intensity visible in the SCS on the ultrasound image was 16.2 ± 4.6 seconds after injection. There were no significant differences among 250-, 500-, and 800-μL contrast volumes injected in time after injection to appearance of the contrast on the ultrasound image (Table 1). In the sagittal ultrasound section, the microbubble contrast agent was visible in a mean 24.0% to 27.2% of the entire SCS when injected with 250, 500, or 800 μL microbubble contrast agents (Table 1). There were no significant differences in area of the SCS where contrast agent was visible among the three volumes injected ($P = 0.90$) or in mean pixel intensity of contrast medium ($P = 0.35$; Fig. 6). Despite only approximately 25% of the SCS having visible contrast, 10 of 12 eyes (83.3%) injected had contrast that reached the posterior pole of the eye (one 250-μL and one 800-μL injection did not, but contrast was observed to extend to approximately two-thirds of the posterior SCS).

Three-Dimensional Ultrasound Contrast Imaging of SCS. As described for 2D ultrasound imaging, in 3D imaging ($n = 4$ eyes) microbubble contrast medium first appeared in

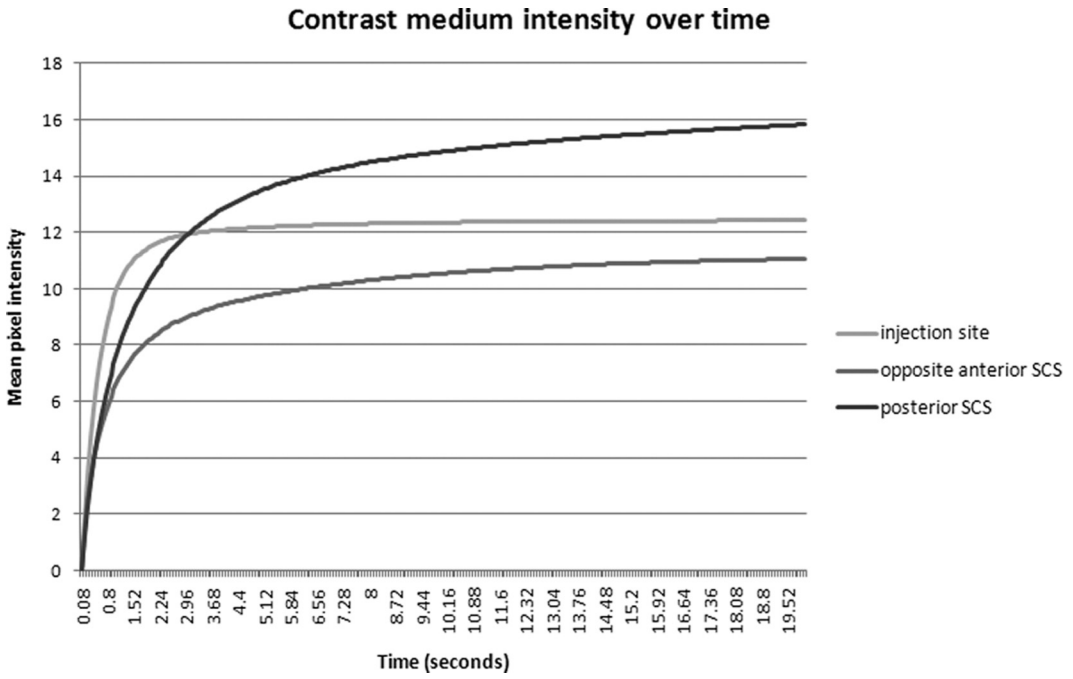

FIGURE 4. Mean pixel intensity representing contrast medium enhancement in regions of interest placed over the injection site, opposite the anterior SCS and the posterior SCS after the injection of 250, 500, and 800 μL microbubble contrast agent into the superoanterior SCS of an ex vivo porcine eye. Measurements of all contrast medium doses are combined in this graph. Contrast enhancement increases rapidly at the injection site, followed by the opposite anterior and posterior SCS.

the SCS at the injection site, then moved to the opposite side of the anterior SCS and into the posterior segment. Contrast agent was uniformly distributed in the anterior SCS, and reached the posterior SCS in all eyes (Fig. 7; Supplementary Movie S2, http://www.iovs.org/lookup/suppl/doi:10.1167/iovs.11-7525/-/DCSupplemental). Median percentage of contrast agent distribution in the entire SCS was 45.3%, with a range of 39.0% to 52.1%.

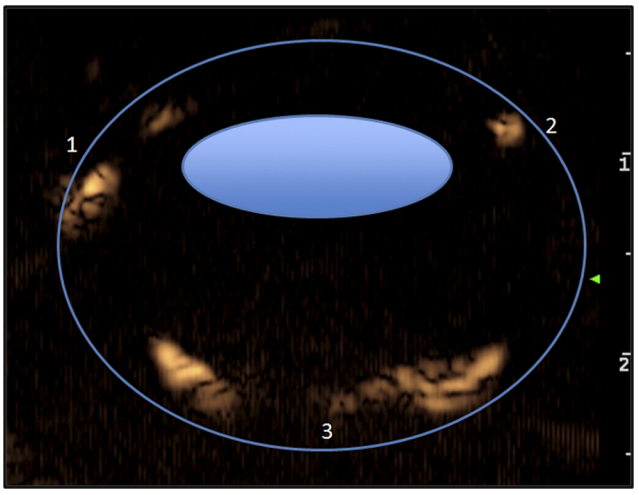

FIGURE 5. Ultrasound image, with overlay of a basic ocular schematic, after injection of 500 μL microbubble contrast agent into the superoanterior SCS of an ex vivo porcine eye. Contrast was visible initially in the SCS at the injection site (1), then visible at the opposite ventral anterior SCS (2) and the posterior SCS (3). An ultrasound system with contrast imaging capabilities was used to image the eyes.

DISCUSSION

A single injection into the anterior SCS resulted in the distribution of latex to nearly 50% of the ocular posterior segment in two large animal species commonly used for retinal research. The SCS was demonstrated to be able to expand, in a dose-dependent manner, to accommodate various volumes of injected fluid. Physiologic IOP did not affect the distension of the SCS after injection, but there was a dose-dependent transient increase in IOP after injection. The clinical and pathologic significance of this transient increase in IOP must be further investigated; however, injections of 500 and 800 μL in eyes with physiologic IOP resulted in acute pressure elevations likely sufficient to damage retinal ganglion cells or the optic nerve.[20,21] The results of this study also demonstrated that it is possible to image the SCS with an ultrasound contrast agent. Furthermore, these results support our hypothesis that a single anterior suprachoroidal injection of a drug with a volume as low as 250 μL can reach the ocular posterior segment in eyes that approximate the size and volume of the human eye. Together our results suggest that injections of 250 μL or less can be accommodated by the SCS, result in only transient relatively modest elevations of IOP, and rapidly extend to a large percentage of the ocular posterior segment. Therefore, further development of SCS injections for treatment of macular disease and other diseases of the posterior segment of the eye is warranted.

Our results are similar to the results from a recent study of the injection of particles into the SCS of ex vivo rabbit eyes. Using specific microneedles, a 15-μL volume of microparticles injected into the anterior SCS resulted in distribution of the particles to approximately 36% of the total circumference of the eye.[22] However, in porcine ex vivo eyes, 35 μL barium sulfate contrast agent particles resulted in only approximately 7% posterior segment distribution, as determined with reconstructed MRI images.[22] Therefore, higher SCS injection vol-

TABLE 1. Two-Dimensional Ultrasound Evaluation of the SCS Using Microbubble Contrast

Volume of Ultrasound Contrast Injected	Time to Opposite Anterior SCS (s)	Time to Posterior SCS (s)	Distribution of SCS (%)	Extension to Posterior Pole
250 μL	12.3 ± 5.9	4.3 ± 1.5	24.0 ± 9.3	3/4 eyes
500 μL	6.0 ± 4.1	9.5 ± 6.0	24.6 ± 9.2	4/4 eyes
800 μL	6.3 ± 2.1	8.5 ± 3.9	27.2 ± 13.2	3/4 eyes
Overall	7.8 ± 4.6	7.7 ± 4.6	25.3 ± 9.8	10/12 eyes

Values are mean ± SD.

umes, as used in our studies, may be required for adequate posterior distribution of medication in larger eyes. What effect these large injection volumes had on the in vivo eye remains to be determined. However, it has been demonstrated that the in vivo rabbit eye can accommodate SCS injections of up to 200 μL sodium hyaluronate or perfluorocarbon gases.[23,24] Therefore, it is likely that the larger canine, porcine, or human eye would also tolerate SCS injection volumes capable of large (200–250 μL) posterior segment distribution.

This study demonstrates that contrast-enhanced ultrasound can be used to determine the dynamic distribution of a single anterior SCS injection in real time. Ultrasound contrast agents are composed of a perfluorocarbon gas core encapsulated by a lipid shell, stabilized by a layer of polyethylene glycol. The microbubbles are suspended in saline at a concentration of approximately 1×10^9 particles/mL, with a median bubble diameter of approximately 2.5 μm.[25] Ultrasound contrast agents may not accurately reflect the flow and distribution of drugs in the SCS because of differences in particle size and viscosity. Microbubbles, because of their gas content, tend to rise to the upper portion of a fluid-filled space, which could alter the distribution of the contrast agent in the SCS when compared with injected medication. However, the porcine eyes in this study were imaged with the anterior SCS facing up, which might have led to an increased accumulation of microbubbles in the anterior SCS and a non–gravity-dependent liquid would be expected to reach the posterior SCS even better. The fact that the ultrasound contrast agent consistently reached the posterior segment is very encouraging for the development of SCS injections for the treatment of ocular posterior segment diseases.

Contrast flow, when observed dynamically in a midsagittal image plane, extended from the injection site in the anterior SCS to the contralateral anterior SCS, indicating flow parallel to the limbus in the anterior SCS. Simultaneously, or in some eyes with a small delay, contrast medium also extended to the posterior SCS. In all eyes the posterior segment was reached by the contrast agent within seconds, confirming that the SCS can be used as a site for drug delivery and that injections of medications into the anterior SCS, the most accessible location of the SCS, will allow distribution of the drug to the posterior targeted tissue. Viscous or microparticle formulations may have different distribution characteristics, but our preliminary studies with latex, PBS, and ultrasound contrast demonstrated rapid distribution into the posterior SCS.

The ability of ultrasound contrast agents to reach the posterior segment of the eye is not only of value when considering the anterior SCS as a site for therapeutic drug administration, it may also be a method for specific drug delivery. Contrast ultrasound-assisted drug delivery has been shown to be feasible both in vivo and in vitro.[26] Binding of pharmaceutical agents to the microbubble shell turns the contrast agent into a vehicle for drug or gene delivery.[27,28] Moreover, a higher energy ultrasound beam can be applied focally in the targeted region, such as the macula, to disrupt microbubbles and cell membranes and locally deliver the drug or gene, thus avoiding the systemic distribution of the substance and potentially reducing the blood-ocular barrier.[29,30]

Three-dimensional contrast-enhanced ultrasound is a novel technology that allows understanding of the pattern of distri-

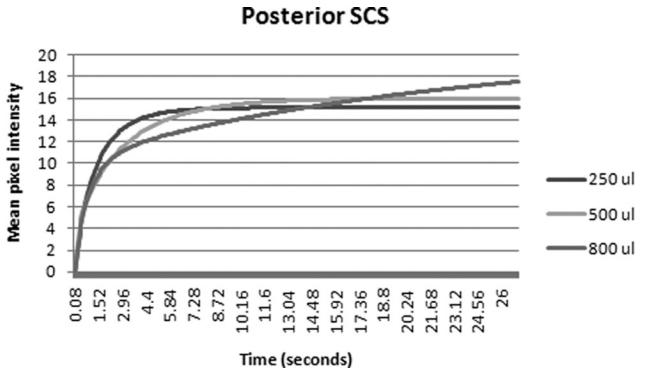

FIGURE 6. Mean pixel intensity representing contrast medium enhancement in regions of interest placed over the posterior SCS after the injection of 250, 500, and 800 μL microbubble contrast agent into the superoanterior SCS of an ex vivo porcine eye. No significant differences in contrast medium enhancement were detected with different doses ($P = 0.35$).

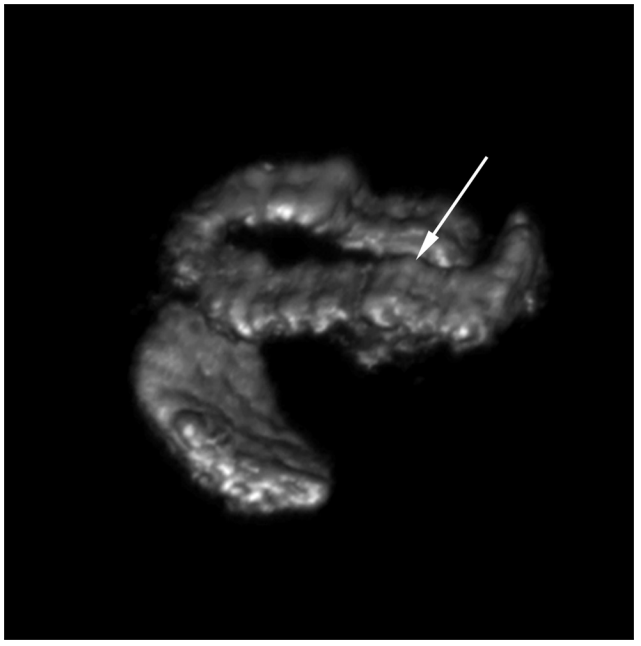

FIGURE 7. Three-dimensional model of contrast agent distribution within the eye. Microbubble contrast agent (250 μL) was injected into the superoanterior SCS of an ex vivo porcine eye, and 3D ultrasound was performed. The contrast agent in the SCS is isolated in this image; no other structures are displayed. The corneal surface faces up in this image. *Arrow*: injection site.

bution of contrast medium in the SCS. Selecting a single two-dimensional image, or even multiple two-dimensional images, for measuring the percentage distribution of contrast agent is prone to underestimation or overestimation of the actual distribution because of the variability of contrast flow within the SCS.[31] This may explain the higher percentage of contrast medium distribution when considering 3D imaging of the entire eye compared to a single slice; 3D imaging was limited to the lowest volume of 250 μL because no statistically significant differences in contrast distribution were detected with 2D imaging performed with different volumes.

These studies represent a novel approach for performing and assessing injections into the anterior SCS and suggest that access to the anterior SCS, either by cannula or microneedles, may allow the distribution of drugs to a large area of the ocular posterior segment and to the macular area of the eye. Additional studies are needed to determine the effect of choroidal blood flow and IOP on the distribution of specific medications and formulations to the retina and macula. Furthermore, contrast ultrasound-assisted drug delivery from SCS injections may represent a novel, targeted, and less invasive method of treatment of ocular posterior segment disease.

References

1. Edelhauser H, Rowe-Rendleman C, Robinson M, et al. Ophthalmic drug delivery systems for the treatment of retinal diseases: basic research to clinical applications. *Invest Ophthalmol Vis Sci.* 2010; 51:5403–5420.
2. Maurice DM. Drug delivery to the posterior segment from drops. *Surv Ophthalmol.* 2002;47(suppl 1):S41–S52.
3. Hughes P, Olejnik O, Chang-Lin J, Wilson C. Topical and systemic drug delivery to the posterior segments. *Adv Drug Deliv Rev.* 2005;57:2010–2032.
4. Lee SS, Hughes PM, Robinson MR. Recent advances in drug delivery systems for treating ocular complications of systemic diseases. *Curr Opin Ophthalmol.* 2009;20:511–519.
5. Kim H, Csaky KG, Gravlin L, et al. Safety and pharmacokinetics of a preservative-free triamcinolone acetonide formulation for intravitreal administration. *Retina.* 2006;26:523–530.
6. Kim S, Galban C, Lutz R, et al. Assessment of subconjunctival and intrascleral drug delivery to the posterior segment using dynamic contrast-enhanced magnetic resonance imaging. *Invest Ophthalmol Vis Sci.* 2007;48:808–814.
7. Kim SH, Lutz RJ, Wang NS, Robinson MR. Transport barriers in transscleral drug delivery for retinal diseases. *Ophthalmic Res.* 2007;39:244–254.
8. Sampat KM, Garg SJ. Complications of intravitreal injections. *Curr Opin Ophthalmol.* 2010;21:178–183.
9. Shima C, Sakaguchi H, Gomi F, et al. Complications in patients after intravitreal injection of bevacizumab. *Acta Ophthalmol.* 2008;86:372–376.
10. Callanan DG, Jaffe GJ, Martin DF, Pearson PA, Comstock TL. Treatment of posterior uveitis with a fluocinolone acetonide implant: three-year clinical trial results. *Arch Ophthalmol.* 2008; 126:1191–1201.
11. Krohn J, Bertelsen T. Corrosion casts of the suprachoroidal space and uveoscleral drainage routes in the human eye. *Acta Ophthalmol Scand.* 1997;75:32–35.
12. Einmahl S, Savoldelli M, D'Hermies F, Tabatabay C, Gurny R, Behar-Cohen F. Evaluation of a novel biomaterial in the suprachoroidal space of the rabbit eye. *Invest Ophthalmol Vis Sci.* 2002; 43:1533–1539.
13. Olsen TW, Feng X, Wabner K, et al. Cannulation of the suprachoroidal space: a novel drug delivery methodology to the posterior segment. *Am J Ophthalmol.* 2006;142:777–787.
14. Hou J, Tao Y, Jiang Y, Wang K. In vivo and in vitro study of suprachoroidal fibrin glue. *Jpn J Ophthalmol.* 2009;53:640–647.
15. Olsen TW, Feng X, Wabner K, et al. Pharmacokinetics of pars plana intravitreal injections versus microcannula suprachoroidal injections of bevacizumab in a porcine model. *Invest Ophthalmol Vis Sci.* 2011;52:4749–4756.
16. Gilger BC, Salmon JH, Wilkie DA, et al. A novel bioerodible deep scleral lamellar cyclosporine implant for uveitis. *Invest Ophthalmol Vis Sci.* 2006;47:2596–2605.
17. Patel S, Lin A, Edelhauser HF, Prausnitz M. Suprachoroidal drug delivery to the back of the eye using hollow microneedles. *Pharm Res.* 2011;28:166–176.
18. Gilger BC, Reeves KA, Salmon JH. Ocular parameters related to drug delivery in the canine and equine eye: aqueous and vitreous humor volume and scleral surface area and thickness. *Vet Ophthalmol.* 2005;8:265–269.
19. Shafiee A, McIntire GL, Sidebotham LC, Ward KW. Experimental determination and allometric prediction of vitreous volume, and retina and lens weights in Gottingen minipigs. *Vet Ophthalmol.* 2008;11:193–196.
20. Bui BV, Edmunds B, Cioffi GA, Fortune B. The gradient of retinal functional changes during acute intraocular pressure elevation. *Invest Ophthalmol Vis Sci.* 2005;46:202–213.
21. Oz O, Gurelik G, Akyurek N, Cinel L, Hondur A. A short duration transient ischemia induces apoptosis in retinal layers: an experimental study in rabbits. *Eur J Ophthalmol.* 2005;15:233–238.
22. Patel SR, Lin AS, Edelhauser HF, Prausnitz MR. Suprachoroidal drug delivery to the back of the eye using hollow microneedles. *Pharm Res.* 2011;28:166–176.
23. Mittl RN. Perfluorocarbon gases in the suprachoroidal space of rabbit eyes. *Graefes Arch Clin Exp Ophthalmol.* 1990;228:589–593.
24. Mittl RN, Tiwari R. Suprachoroidal injection of sodium hyaluronate as an 'internal' buckling procedure. *Ophthalmic Res.* 1987;19: 255–260.
25. Rychak JJ, Graba J, Cheung AM, et al. Microultrasound molecular imaging of vascular endothelial growth factor receptor 2 in a mouse model of tumor angiogenesis. *Mol Imaging.* 2007;6:289–296.
26. Klibanov AL. Microbubble contrast agents: targeted ultrasound imaging and ultrasound-assisted drug-delivery applications. *Invest Radiol.* 2006;41:354–362.
27. Burke CW, Price RJ. Contrast ultrasound targeted treatment of gliomas in mice via drug-bearing nanoparticle delivery and microvascular ablation. *J Vis Exp.* 2010;46: pii: 2145. doi: 10.3791/2145.
28. Uesugi Y, Kawata H, Jo J, Saito Y, Tabata Y. An ultrasound-responsive nano delivery system of tissue-type plasminogen activator for thrombolytic therapy. *J Control Release.* 2010;147:269–277.
29. Hynynen K. Focused ultrasound for blood-brain disruption and delivery of therapeutic molecules into the brain. *Expert Opin Drug Deliv.* 2007;4:27–35.
30. Lum AF, Borden MA, Dayton PA, Kruse DE, Simon SI, Ferrara KW. Ultrasound radiation force enables targeted deposition of model drug carriers loaded on microbubbles. *J Control Release.* 2006; 111:128–134.
31. Feingold S, Gessner R, Guracar IM, Dayton PA. Quantitative volumetric perfusion mapping of the microvasculature using contrast ultrasound. *Invest Radiol.* 2010;45:669–674.